# Characterization of a Fluidized-Bed Plasma Reactor

**Craig R. Wierenga**
**Terrence J. Morin**
Department of Chemical Engineering
University of Idaho
Moscow, ID 83843

Chemical synthesis and material processing in the highly reactive environment of a gas plasma has been a fertile field of research. The plasma state is well suited to such applications, as the ionized gas may be both an energy transfer medium and a source of reactive intermediates. The wide variety in the literature is due not only to the vast array of chemical systems of interest, but also to the manifold methods of plasma operation and plasma-solid contacting. Historically, many of the difficulties in effecting plasma-solid reactions have been related to the contacting schemes employed.

The plasma-fluidized-bed reactor (PFBR) has been designed to effect the fluidized-bed contacting of a nonequilibrium gas plasma with granular solid material. The reactor is a solids bed fluidized by a subatmospheric pressure, high-frequency (2.45 GHz) plasma within a cylindrical cavity resonator. The PFBR takes advantage of many of the properties of conventional gas fluidized-bed reactors, as, for example, well-mixed solids, isothermal operation, good temperature control, and fluid-like properties of the bed. Although fluid-bed contacting between solids and the tail region of a d.c. or r.f. plasma has been used for rapid quenching of the plasma jet (Goldberger and Oxley, 1963) as well as to effect spouted beds (Jurewicz, et al. 1985), the PFBR is unique in that it involves contact of solids with the active or current-carrying portion of the plasma in a fluidized bed.

The first of two objectives of this work is to demonstrate "proof of concept" of the PFBR, that is, to establish that it is possible to ionize the interstitial, intraslug, and intrabubble regions of a gas fluidized bed and to maintain such a reactor in steady operation.

Given the first objective, the second is the characterization of the properties of the PFBR as a fluidized bed and as a plasma reactor over ranges of gas, solid, and microwave cavity conditions. These characterization studies involve inert gases and solids and the results are compared with similar studies of laboratory fluidized beds involving nonionized gases. It is expected that the presence of electromagnetic fields and attendant heating processes alter the fluidization process. Contemporary views of bubble formation and bed stabilization include a role for interparticle forces as well as for hydrodynamic forces (Yates, 1983). One would expect that the presence of an ionized fluidizing agent would strongly influence the nature and strength of the interparticle forces, and therefore alter the bed behavior. The recent work of Moissis and Zahn (1988) indicates that even without an ionized fluidizing gas, the presence of a high frequency electromagnetic field can result in bed stabilization and suppression of bubble formation.

Correspondence concerning this paper should be addressed to T. J. Morin.

## Apparatus

The laboratory apparatus used in this investigation, shown schematically in Figure 1, consists of three main circuits. The power circuit includes the microwave generator, transmission lines, and the resonant cavity. The gas-handling circuit is made up of the reactor, gas-delivery system, and the vacuum/exhaust equipment. The third circuit is the water and air cooling system for the cavity and reactor. Each of these circuits has associated measurement devices, and will be discussed in detail below.

From a 0–500-W generator operating at 2.45 GHz, the microwave signal is transmitted through a combination of WR284 waveguide and 7/8-inch EIA air-dielectric coaxial cable. The waveguide circuit includes a three-port circulator with a water cooled dummy load to protect the magnetron from large reflected power levels. A directional coupler with 50-db forward and 45-dB reflected attenuation is included for power measurements. The microwave signal is coupled to the plasma by a resonant cavity similar to the one described by Morin, et al. (1989). The cavity may be operated in several resonant modes (see, for example, Harrington, 1961). The reactor is mounted coaxially with the resonant cavity. With the modes used in this study, the areas of high electrical field strength are located along the axis of the cavity.

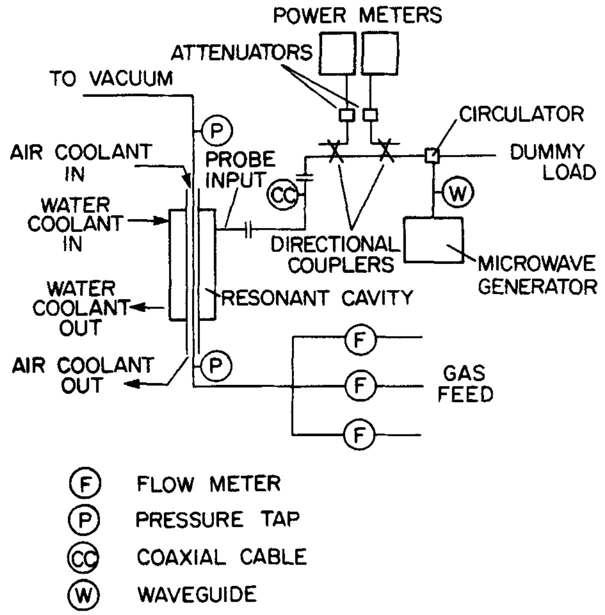


**Figure 1. Gas flow, microwave power, and cooling circuits for PFBR.**

Pressure measurements are made in two locations. The upstream tap is at the bottom of the reactor, just above the gas inlet, and approximately 0.46 m below the porous distributor. The downstream tap is at the top of the reactor, about 0.25 m above the bed. Ideally, these taps should be located directly adjacent to the bed, but the friction drop through such a short length of smooth glass tubing is insignificant with respect to the pressure drop through the glass frit and solids bed. The pressure drop through the frit was measured over the range of experimental conditions and in the absence of the bed. The measurements, and Darcy's law for flow of a compressible fluid through a porous solid were used to construct an empirical function for the pressure drop.

The glass reactor and the brass cavity are jacketed and cooled with air and water streams, respectively.

## Results

Resonantly sustained electromagnetic standing waves routinely produced interstitial, intrabubble and intraslug plasmas in a fluidized bed of glass beads, with bead diameters of 0.17 to 3 mm. Bed diameters of 10 and 20 mm were fluidized with both argon and hydrogen plasmas at pressures ranging from 100 to 6,600 Pa. Gas flow rates varied such that the bed condition ranged from fixed to violently slugging. While four resonant modes were supported in either hydrogen or argon or both, the $TM_{012}$ cylindrical cavity mode was found to be the best, in terms of operational ease and axial location of the high electric field strengths.

In addition to the presence of glowing bubbles in a fluidized bed, there are several other features of the PFBR observed in the course of the work. The centerline temperature of the bed often became great enough to melt the glass beads and fuse them together. This behavior was a function of power level, pressure, flow rate, particle diameter, and fluidizing gas. Limited experimentation with ilmenite ($TiFeO_3$) as the bed material, produced similar results. As the melting point of ilmenite is above 2,000 K, it appears that the PFBR is capable of generating temperatures of that magnitude. The formation of clinkers was dramatically reduced or eliminated after transition from a fixed to a fluidized bed.

A feature common to both the fixed-bed and fluidized-bed plasma reactors is the presence of both diffuse glows and filamentary arcs. The arcs were observed at higher pressures, with the threshold pressure for arc formation varying with the gas composition.

The focus of the characterization studies includes both the fixed- and fluid-bed operation of the plasma reactor, and they attempt to identify, both quantitatively and qualitatively, the significant features of the plasma fluidized-bed reactor. The range of experimental variables is described in Table 1.

The characterization studies involve operation of the bed in both fixed-bed and fluid-bed regime. The results reported here are primarily those from the fluid-bed regime, with a few necessary exceptions. The fixed-bed results appear separately (Wierenga, 1989).

The particle Knudsen number, $Kn_p$, is included in Table 1 in order to emphasize that a continuum description of the fluid flow is appropriate. In one of the few treatments of vacuum fluidization, Germain and Claudel (1976) made use of continuum flow pressure drop relations to successfully predict gas flow rates and pressure drops in low pressure (500–4,000 Pa), fixed and fluidized beds of glass spheres. The predictions of two conventional minimum fluidization velocity correlations were compared to the results of plasma-free bed operation. One of the most widely accepted correlations, that of Wen and Yu (1966), has been validated for Reynolds numbers ranging from 0.001 to 4,000.

$$Re_p = (33.7 + 0.0408\ Ga)^{1/2} - 33.7 \qquad (1)$$

Though the data from this work falls in the very low end of this range, the correlation was found to agree with the experimental values of $U_{mf}$. Actual deviations ranged from 2 to 30%, which is generally considered to be good agreement for minimum fluidization velocity calculations. The low Reynolds number correlation of Geldart (1973) gave a similar correspondence. It should be noted that these comparisons were based upon the nonplasma data only. These experiments were carried out in an attempt to provide a base case of conventional fluidization data for comparison to the unknown behavior of a plasma fluidized bed.

An important, but uncertain, factor in the characterization of the PFBR is the temperature profile in the bed. The temperature is important in calculation of the gas superficial velocity,

**Table 1. Summary of Experimental Design**

| Variable | Value |
|---|---|
| Gas Composition | Argon<br>Hydrogen |
| Solid Composition | Glass Spheres |
| Sphere Dia., $d_p \cdot$mm | 0.17–0.18<br>0.25–0.30<br>0.45–0.50 |
| Freeboard pres., Pa | 266, 1,330, 2,000, 2,660 |
| Microwave Power Density, W/cm³ | 0–30* |
| $Re_{p,mf}$ | 0.004–0.2 |
| $Kn_p$ | <0.05 |

*Power density = power absorbed vs. void volume of bed.

Table 2a. Temperatures for an Argon Fluidized Plasma Reactor

| Pressure Pa | $d_p$, m | Power Density W/cm³ | Temp. K |
|---|---|---|---|
| 266 | 0.00025 | 12.6 | 375 |
| | | 17.7 | 425 |
| | 0.00045 | 11.5 | 500 |
| | | 27.4 | 750 |
| 1,330 | 0.00017 | 11.6 | 375 |
| | | 20.7 | 450 |
| | 0.00025 | 11.5 | 460 |
| | | 15.7 | 450 |
| | 0.00045 | 10.5 | 450 |
| | | 30.9 | 700 |
| 2,000 | 0.00017 | 10.8 | 375 |
| | 0.00025 | 14.0 | 500 |
| | | 16.8 | 475 |
| | 0.00045 | 10.9 | 450 |
| | | 30.8 | 750 |
| 2,660 | 0.00017 | 12.0 | 375 |
| | 0.00025 | 12.4 | 575 |
| | | 15.2 | 450 |
| | 0.00045 | 10.8 | 375 |
| | | 30.5 | 900 |

gas density, and gas viscosity. The bed temperature is uncertain, due to the electromagnetically hostile environment of the resonant cavity. An indirect method was applied in order to infer an average bed temperature from fixed-bed regime pressure-drop measurements. An iterative procedure using the Ergun (1952) equation for pressure drop through fixed beds was used to infer the temperature. Given a mass flow rate at standard conditions and the corresponding pressure drop across the bed, the temperature was used as a parameter to fit the Ergun equation to the data. The average bed temperatures calculated in this manner ranged from 350 to 900 K, and are summarized in Table 2. Note from Table 2 that the inferred average bed temperature increases with both pressure and power level, and that the same pressure and power level, the temperatures of the beds fluidized in hydrogen are higher than those fluidized in argon. Figure 2 illustrates the thermal effects of a plasma on fixed-bed behavior. Note that as pressure, and hence temperature, increases, the slope of the fixed-bed data becomes steeper. This is exactly the behavior predicted by the Ergun equation and is a consequence of the temperature dependence of the gas viscosity.

There are two important assumptions involved in this temperature estimation procedure. The first is that, for a given pressure and microwave power level, the fixed-bed and fluid-bed temperatures are identical. This assumption is a reasonable one given the low density of the fluidizing gas. The second assumption is that the Ergun equation is an appropriate description of flow of a weakly ionized gas in a fixed bed. The Ergun equation does not include electrophoretic effects in the analysis of momentum transfer. Although such effects are likely to be present in the fixed- and fluidized-bed plasma reactors, a review by Chanin (1978) indicates that electrophoretically-induced pressure gradients in capillary tubes are on the order of 10 Pa/m or less. The pressure gradients associated with gas velocities of 0.1–2.0 m/s through glass frits and beds are at least an order of magnitude larger than this.

Table 2b. Temperatures Inferred for a Hydrogen Fluidized Plasma Reactor

| Pressure Pa | $d_p$, m | Power Density W/cm³ | Temp. K |
|---|---|---|---|
| 266 | 0.00017 | 16.0 | 375 |
| | 0.00025 | 14.6 | 375 |
| | 0.00045 | 14.0 | 350 |
| | | 33.0 | 500 |
| 1,330 | 0.00045 | 16.1 | 500 |
| | | 34.9 | 900 |
| 2,000 | 0.00045 | 16.0 | 500 |
| | | 39.0 | 650 |
| 2,660 | 0.00045 | 15.7 | 550 |

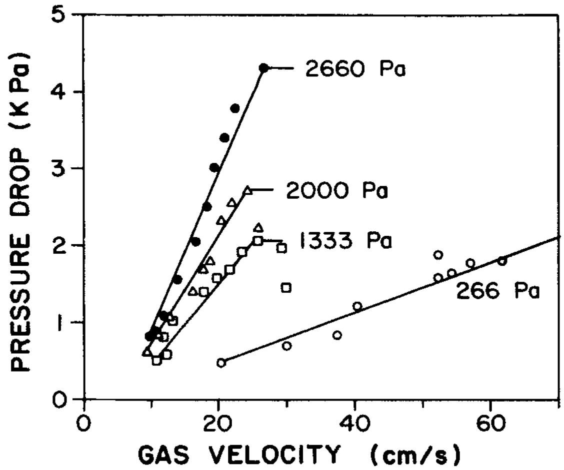


**Figure 2. Pressure drop through 4-cm bed of 0.45-mm glass spheres in the presence of argon plasma. Power density = 29.9 W/cm³**

The dependence of $U_{mf}$ on particle size, $d_p$, and inferred bed temperature, is described in Table 3. In both the plasma- and nonplasma-fluidized bed, minimum fluidization velocity, $U_{mf}$, increases as particle diameter increases. The Geldart correlation (Geldart, 1973) for low $Re_p$ fluidization predicts that $U_{mf}$ should vary with the 1.8th power of particle diameter. The experimental data from the gas-fluidized bed agrees with this prediction, with the exponent of $d_p$ ranging from 1.75 for argon, to 1.87 for hydrogen. For a bed fluidized with ionized argon, the minimum

Table 3. Minimum Fluidization Velocities and Inferred Gas Temperatures for Argon and Hydrogen Plasma Fluidized Beds

| Gas | P, Pa | T, K | Meas. $U_{mf}$ cm/s | Predicted $U_{mf}$ cm/s |
|---|---|---|---|---|
| *Hydrogen* | 2,000 | 300 | 49.0 | 60.0 |
| | | 500 | 65.0 | 44.0 |
| | | 650 | 85.0 | 36.0 |
| *Argon* | 266 | 300 | 17.0 | 23.0 |
| | | 500 | 27.0 | 18.0 |
| | | 750 | 57.5 | 13.0 |
| | 1,333 | 300 | 22.5 | 23.0 |
| | | 450 | 25.0 | 18.0 |
| | | 700 | 26.0 | 13.0 |
| | 2,000 | 300 | 21.0 | 23.0 |
| | | 450 | 26.5 | 18.0 |
| | | 750 | 24.0 | 13.0 |

Glass spheres: 0.45 mm diameter

fluidization with ionized argon, the minimum fluidization velocity is proportional to the 2.24th power of particle diameter. It is possible that the electromagnetic fields associated with the resonant cavity affect the fluidization behavior, and if so, the effect could be in the form of enhanced interparticle polarization forces, which are a function of particle size.

The dependence of the value of $U_{mf}$ on bed temperature, as predicted by the correlation of Wen and Yu (1966), is included in Table 3. This trend of decreasing $U_{mf}$ as temperature increases has also been reported by Pattipati and Wen (1981). Their work demonstrated that for sand particles less than 2 mm in diameter and fluidized with air, $U_{mf}$ decreased with increasing temperature. Both basic plasma theory and experimental observations made in the course of this study affirm that the temperature in the plasma is higher than in the nonionized gas. Thus, one would expect the minimum fluidization velocity of a plasma-fluidized bed to be less than that of the corresponding gas-fluidized bed, because of the aforementioned thermal effect. The observed trend in almost all of the current data, however, was exactly opposite. In fact, the only exceptions were in those experiments where the difference between plasma and nonplasma $U_{mf}$ was so small as to be indistinguishable from experimental error. In light of the earlier discussion of $U_{mf}$ vs. $d_p$ behavior, the most probable explanation of these unexpected results is that interparticle forces play a more significant role in plasma fluidization than in conventional systems. These interparticle forces could be enhanced by heat softening and subsequent adhesion of the glass beads, but, as clinker formation was minimal, the enhancement is more likely an electromagnetic effect.

## Acknowledgments

Support for this work was provided by the National Science Foundation under Grant #CBT-8706899. The authors would like to thank Mr. Thomas Rogers for preparation of the artwork.

## Notation

$d_p$ = diameter of glass bead, m
$Ga$ = Galileo number
$Kn_p$ = Knudsen number
$Re_{p,mf}$ = Reynolds number at minimum fluidization
$U_{mf}$ = superficial velocity at minimum fluidization, m/s

## Literature Cited

Jurewicz, J., P. Proulx, and M. Boulos, "The Plasma Spouted Bed Reactor," p. 243, Proc. of 7th Int. Symp. on Plasma Chem., Eindhoven, (1985).

Chanin, L. M., "Nonuniformities in Glow Discharges: Electrophoresis," part 2.3 of *Gaseous Electronics*, vol. I, ed., H. J. Oskam, Academic Press, Orlando (1978).

Ergun, S., "Fluid Flow Through Packed Columns," *Chem. Eng. Prog.*, **48**(2), 89 (1952).

Geldart, D., "Types Of Gas Fluidization," *Powder Tech.*, **7**, 285 (1973).

Germain, B., and B. Glaudel, "Fluidization at Mean Pressures Less than 30 Torr," *Powder Tech.*, **13**, 115 (1976).

Goldberger, W. M., and J. H. Oxley, "Quenching The Plasma Reaction by Means of the Fluidized Bed," *AIChE J.*, **9**, 778 (Sept., 1963).

Harrington, R. F., *Time-Harmonic Elecgtromagnetic Fields*, ch. 5, McGraw-Hill, New York (1961).

Moissis, A. A., and M. Zahn, "Boundary Value Problems in Electrofluidized and Magnetically Stabilized Beds," *Chem. Eng. Comm.*, **67**, 181 (1988).

Morin, T. J., R. Chapman, and M. C. Hawley, "Flow Calorimetry of Electrical Discharges," *Chem. Eng. Comm.*, **73**, 183 (1989).

Pattipati, R. R., and C. Y. Wen, "Minimum Fluidization Velocity at High Temperatures," *Ind. Eng. Chem. Proc. Des. Dev.*, **20**, 705 (1981).

Wen, C. Y., and Y. H. Yu, "Fluid Particle Technology," *AIChE Symp. Ser.*, **62**(62), 100 (1966).

Wierenga, C. R., "Development and Characterization of a Plasma Fluidized Bed Reactor," MS thesis, University of Idaho (1988).

Yates, J. G., *Fundamentals of Fluidized-Bed Chemical Processes*, Butterworths, London (1983).

*Manuscript received Feb. 7, 1989, and revision received June 7, 1989.*